Salvador Rubio, FJ.; Gimeno García, J.; Morena Borja, JDL.; Carreres Talens, M. (2012). Using one-dimensional modeling to analyze the influence of the use of biodiesels on the dynamic behavior of solenoid-operated injectors in common rail systems: Results of the simulations and discussion. Energy Conversion and Management. 54(1):122-132. doi:10.1016/j.enconman.2011.10.007.

Energy Conversion and Management 54 (2012) 122–132

USING ONE-DIMENSIONAL MODELLING TO ANALYSE THE INFLUENCE OF THE USE OF BIODIESELS ON THE DYNAMIC BEHAVIOR OF SOLENOID- OPERATED INJECTORS IN COMMON RAIL SYSTEMS: RESULTS OF THE SIMULATIONS AND DISCUSSION

F. J. Salvador (*), J. Gimeno, J. De la Morena, M. Carreres

CMT-Motores Térmicos. Universitat Politècnica de València, Spain

Camino de Vera s/n, E-46022 Spain.

(*) Corresponding author:

Dr. Javier Salvador, fsalvado@mot.upv.es

CMT-Motores Térmicos, Universitat Politècnica de València

Camino de Vera s/n, E-46022 Spain.

Telephone: +34-963879659

FAX: +34-963877659

ABSTRACT

The influence of using biodiesel fuels on the hydraulic behavior of a solenoid operated common rail injection system has been explored by means of a one-dimensional model. This model has been previously obtained, including a complete characterization of the different components of the injector (mainly the nozzle, the injector holder and the electrovalve), and extensively validated by means of mass flow rate results under different conditions. After that, both single and multiple injection strategies have been analyzed, using a standard diesel fuel and rapeseed methyl ester (RME) as working fluids. Single long injections allowed the characterization of the hydraulic delay of the injector, the needle dynamics and the discharge capability of the couple injector-nozzle for the two fuels considered. Meanwhile, the effect of biodiesel on main plus post injection strategies has been evaluated in several aspects, such as the separation of the two injections or the effect of the main injection on the post injection fueling. Finally, a modification in the injector hardware has been proposed in order to have similar performances using biodiesel as the original injector configuration using standard diesel fuel.

KEYWORDS: injector, modelling, biodiesel, diesel, dynamic

NOMENCLATURE

A_o	Geometrical outlet nozzle area
C_d	Discharge coefficient
D_o	Geometrical nozzle diameter

D_{OA}	Diameter of the outlet orifice of the control volume
$\dot{m}_f$	Mass flow
P_{inj}	Injection pressure
u_B	Theoretical velocity, $u_B = \sqrt{\frac{2 \cdot \Delta P}{\rho_f}}$
	Greek Symbols
ΔP	Pressure drop, $\Delta P = P_{inj} - P_b$
ρ_f	Fuel density
υ_f	Kinematic viscosity

1. INTRODUCTION

Significant efforts have been made by the automotive industry in order to reduce the environmental impact of engines along the past years. For this purpose, several strategies have been considered and analyzed. For example, the use of multiple injections has shown a potential to modify the combustion development and reduce the pollutant formation [1]-[3]. Beside this, the influence of alternative fuels (especially biofuels derived from vegetable oils) on pollutant emissions and engine performance has been widely studied [4]-[9]. Lapuerta *et al.* [10] have recently made a review of these studies, leading to the following conclusions:

- At full load conditions, lower power is obtained when running the engine with biodiesel fuels, due to their lower heating value.

- Nitrogen oxides emissions are slightly higher for biodiesel fuels in general terms.
- Soot generation and emission is considerably reduced due to the higher oxygen content and the absence of aromatic components.

Anyway, most of these studies treat the engine like a “black box”, comparing standard fuel and biodiesel (pure or blended) mainly in terms of emissions and performance, but not paying attention to the particular effects of using biodiesel fuels on the different specific phenomena involved in engine combustion. For this reason, there are still important uncertainties with respect to the influence of using biofuels on the hydraulic behavior of injection systems. One-dimensional approaches have demonstrated their ability to reproduce the discharge characteristic of diesel injectors once they are completely characterized [11]-[13]. Beside this, different investigations have been carried out with standard diesel fuels to characterize nozzle flow, spray behavior and combustion process, seeing that there is a significant interaction between the hydraulic behavior of the injection system and posterior phenomena such as air-fuel mixing process or pollutant formation [14]-[20].

In the current work, a study about the influence of a biodiesel fuel on the hydraulic characteristics of a standard diesel injection system has been carried out. In the first part of this study, a one dimensional model of a second generation solenoid injector has been developed in the code AmeSim and extensively validated [21]. For this purpose, a detailed dimensional and hydraulic characterization of the different elements that compose the injector has been done.

Afterwards, in the current paper, this one-dimensional model will be evaluated using standard diesel and rapeseed methyl ester fuels and two kinds of injection strategies:

single injection and main plus post injection. For the single injection strategy the performance of the injection system will be compared principally in terms of its dynamic response, the flow capability at stationary conditions and the hydraulic delay between the command signal and the start of injection. Regarding the multiple injection analysis, the study will be focused on the effect of fuel properties on the interaction between the main and the post injection at different dwell times. Additionally, the influence of the fuel properties (mainly bulk modulus and speed of sound) on the behavior of the pressure waves at the nozzle inlet will be studied. Finally, a modification in the control volume geometry will be proposed, so that the differences seen in the needle dynamics when using biodiesel fuel are reduced, giving a similar behavior as the original injection system with standard diesel fuel.

As far as the structure of the paper is concerned, this study is divided in five sections. Firstly, in section 2 the injector model is introduced. After this, in section 3, the analysis of single injection strategies will be performed, in order to compare the needle dynamics and the stationary mass flow rate between the diesel and biodiesel fuels. In section 4 the effect of the fuels properties on the injection system performance for multiple injections will be analyzed. Section 5 includes the modification proposed to improve the dynamic behavior of the injector when using biodiesel fuel, which will be described and validated for different injection pressures. Finally, the most important conclusions obtained along the paper will be pointed out in section 6.

2. DESCRIPTION OF THE INJECTOR MODEL

For this study, a one-dimensional model of a solenoid injector has been developed in AmeSim. This model mainly consists of three different parts: the injection holder, the electrovalve and the nozzle. A scheme of each of these parts can be seen in Figure 1.

In order to reproduce an accurate behavior with the injector model, each one of its internal elements needs to be geometrically and hydraulically characterized. To obtain the geometry of these elements, a silicone moulding technique [22] together with Scanning Electron Microscopy (SEM) images has been used. This technique has proved to be useful to obtain the geometry of different components with a significant degree of accuracy. Additionally, purpose-made test rigs have been manufactured and used in order to characterize the hydraulic behavior of the most significant orifices of the injector, such as the ones corresponding to the control volume or the nozzle.

Figure 2 shows the comparison between experimental mass flow rate curves and the results of the injector model for three different injection pressures (30, 80 and 130 MPa) and four energizing times (0.24, 0.5, 1 and 2 ms). As it can be seen, the model reproduces accurately both the mass flow rate shape and the total injected mass during each injection in all the conditions tested. More details of the model and its validation can be seen in Payri, R. et al [21].

3. SINGLE INJECTION ANALYSIS

In this section, a wide study of the performance of the injection system model described in [21] will be carried out. Two fuels are chosen for this study: standard diesel and rapeseed methyl ester, which is one of the most usual biodiesels existing in the literature. As it can be seen in Table 1, biodiesel fuel has significantly higher values of density and viscosity with respect to the standard diesel fuel, so that differences are expected in their hydraulic behavior, both in terms of transient behavior and stationary mass flow rate. Additionally, information about the bulk modulus and the speed of sound of the fuels is shown in Figure 3. As it can be seen, the values of these parameters are considerably similar for the two fuels.

For the single injection characterization, the test matrix includes 6 different injection pressure levels (40, 50, 80, 120, 150 and 180 MPa) evaluated at a fixed chamber pressure of 4 MPa. Energizing times will also be varied (0.4, 0.5, 1 and 2 ms).

3.1. Transient analysis

Firstly, an analysis of the influence of the biodiesel fuel on the transient development of the injection system will be made. Figure 4 represents the temporal evolution of needle lift and mass flow rate for an injection pressure of 40 MPa and different energizing times. It can be clearly seen that the needle velocity during the opening is significantly lower for the biodiesel fuel. Thus, the needle needs higher time to reach its maximum lift with respect to the standard diesel fuel. This fact can be explained in terms of the higher viscosity of the biodiesel fuel, which increases the friction force, affecting the needle dynamics.

As a consequence of the differences observed in terms of needle dynamics, an important effect of fuel properties on the mass flow rate behavior can be observed, especially at the first stages of the injection process. It can be seen that due to the slower needle dynamics the mass flow rate is lower for the RME, especially during the opening slope of the curve. Thus, the amount of mass injected at short energizing times (typical for pilot and post injections) is extremely lower for the biodiesel fuel. When injection pressure gets higher (Figures 5 and 6) the differences observed between the fuels become less important (almost negligible in the case of P_{inj} = 180 MPa), although the same tendencies can be found.

Figure 7.a represents the evolution of the total injected mass against energizing time for the same cases studied before. As it was expected, in all the cases it can be seen that the injected mass increases linearly with ET. Again, for the low injection pressure value (40

MPa) the curve corresponding to the biodiesel fuel is considerably lower than the diesel one, whereas the behavior of the two fuels gets almost equal when injection pressure gets higher.

Apart from the needle velocity and the mass flow rate, it is important to compare the effect of fuel properties on the hydraulic delay. This parameter is defined as the time needed for the injector to start the injection process after receiving the command electric signal from the ECU. The differences between the hydraulic delay of the biodiesel fuel and the regular diesel fuel are depicted in Figure 7.b against the injection pressure. As it can be seen, this difference is extremely higher for the case of P_{inj} = 40 MPa, so that the start of injection occurs considerably later for the RME (~160 μs). Thus, at low injection pressure conditions the ECU should send the signal to the injection considerably earlier if the system is running with RME instead of the standard diesel fuel configuration, in order to start the injection process at the same crankshaft angle. Nevertheless, the hydraulic delay decreases up to 15 or 20 microseconds for higher injection pressures, since the needle movement is much faster and so less affected by the viscous effects.

3.2. Steady-state behavior

Paying attention to the 2 milliseconds injection events it can be seen that the mass flow rate values at full needle lift conditions are slightly higher for the RME fuel. This mass flow rate can be defined as a function of density as:

$$\dot{m}_f = C_d \rho_f A_o u_B = C_d A_o \sqrt{2\rho_f \Delta P} \quad (1)$$

being $\dot{m}_f$ the stationary mass flow rate, C_d the discharge coefficient, ρ_f the fuel density, A_o the section of the outlet hole of the nozzle, u_B the theoretical velocity obtained from

Bernoulli equation and ΔP the difference between injection and discharge pressure. Considering this formula and the fluid density seen in Table 1, differences of around 2.5% would be expected between the fuels in terms of stationary mass flow rate, which nevertheless is not the situation observed in the previous figures.

In order to explain this apparent contradiction, the evolution of the discharge coefficient with respect to Reynolds number will be studied. The Reynolds number is defined as:

$$Re = \frac{D_o u_B}{\nu_f} \tag{2}$$

where D_o is the outlet hole diameter of the nozzle and ν_f is the kinematic viscosity of the fuel.

This information is represented in Figure 8. As expected from previous studies in the literature, the data coming from the different fuels collapse in a single asymptotic curve, whose characteristics depend on the geometry of the nozzle [23]. Nevertheless, it can be seen that, for the same injection conditions, Reynolds number is significantly lower for the biodiesel fuel due to the effect of viscosity. Since the discharge coefficient tends to increase as *Re* gets higher, this value is higher for the regular diesel fuel, so that the effect of the density in equation (1) is partially compensated by the differences in terms of C_d, especially at low injection pressure conditions.

4. MULTIPLE INJECTION ANALYSIS

The influence of the use of biodiesel on the hydraulic performance of the injector under multiple injection strategies is examined in this section. For this purpose, main plus post injections are considered, paying special attention to the effect of the main injection on the second one. To see this influence, different electric dwell times have been tested. The injection conditions selected are the same ones as for the single injection strategies,

studied before, considering energizing times of 1 ms for the main injection and 0.35 ms for the post injection.

4.1. Determination of critical electric dwell time

Mass flow rate behavior at injection pressures of 40 and 180 MPa is shown in Figures 9 and 10 respectively for the standard diesel fuel and the RME. In most of the cases studied, it can be seen that below a certain value of electric dwell time, main and post injections are overlapped, and so, it is impossible to distinguish one injection event from the other. After this critical dwell time, two separate injections are obtained. With respect to the comparison between diesel and biodiesel fuels, it is noticeable that for the case of 40 MPa the post injections start at higher times for the biodiesel fuel, inducing no overlapping, and produce lower amounts of fuel delivered, due to the effect of fuel viscosity on needle dynamics. On the contrary, when injection pressure gets higher this influence decreases, and the two plots are considerably similar.

The characteristic time at which main and post injection mass flow rate signals stop being overlapped can be estimated for each fuel and injection pressure. This information is depicted in Figure 11 against injection pressure. As it can be seen, this time is very similar for the two fuels when injection pressure is higher than 80 MPa. Meanwhile, the behavior of this parameter is completely different for lower injection pressure values. For example, for the case of 40 MPa, post injection mass flow rate curves are separated from the main injection even at the lowest values of electric dwell time, as seen before; on the contrary, when injecting standard diesel the overlapping phenomenon previously described exists, leading to a considerably high critical electric dwell time (around 650 μs). In the case of P_{inj}=50 MPa the overlapping phenomenon exists for the two fuels, although the difference in the critical time between them is considerably high. This

different behavior between the fuels can be explained paying attention to Figure 4: as it can be seen, for the case of ET = 1ms (same as the one used in this study for the main injection), the maximum needle lift reached when using the biodiesel fuel at low injection pressure is significantly lower. Thus, the time needed for the needle to achieve its lowest position after the ET is also shorter for the biodiesel fuel. Additionally, it has been previously seen that the hydraulic delay is larger for the RME, which is also true for the post injection. As a consequence of these facts, for the same injection configuration (injection and back pressures, energizing times and electric dwell time) using the biodiesel fuel implies that the needle closes earlier for the main injection, and starts moving again later for the post injection, so that the separation between the two injection events is higher, needing lower dwell times to get independent injections. Nevertheless, it has to be taken into account that the mass injected during the main and post injections for the biodiesel fuel at low injection pressures is very low, so that higher ET would be needed to achieve the same mass injected, compensating this phenomenon. On the contrary, when injection pressure gets higher, the influence of fuel properties on needle movement gets less significant, so that the critical dwell time becomes similar for the two fuels, as it can be seen in Figure 11.

4.2. Interaction between main and post injection

Another aspect suitable to be studied is the effect of the main injection on the second injection event. One way to analyze this phenomenon is to quantify the mass injected by the post injection for different dwell time values. This procedure has only been done for the dwell times at which main and post injections are completely separated (*i.e.*, dwell times higher than the critical one). The results obtained are shown in Figure 12 for three different injection pressures (50, 80 and 180 MPa). As it can be observed, for short dwell times the post injection mass is clearly affected by the main injection. After a

certain value of DT the mass injected in the post injection is almost independent of the dwell time.

Comparing the fuels, the evolution of the curves is considerably similar for them, especially as injection pressure increases. Nevertheless, it can be observed that the amount of fuel injected during the post injection is strongly higher for the regular diesel fuel in any case. This is due to the better dynamic response of the injection when using this fuel, especially at low energizing times as it is the case in the post injections: the needle opens faster and reaches a higher needle lift, as previously seen in the single injection analysis. Furthermore, the relative difference seen between the two fuels decreases with injection pressure (approximately 150% for P_{inj} = 50 MPa, 75% for P_{inj} = 80 MPa and 20 % for P_{inj} = 180 MPa) due to the fact that the influence of fuel properties on needle dynamics is less important as P_{inj} gets higher, as observed before.

4.3. Study of pressure oscillations

Another important aspect that can be studied is the effect of fuel properties on the pressure waves existing in the injector and the nozzle. These pressure oscillations are generated during the opening and closing phases of the injection event, and their behavior is mainly dependent on the bulk modulus and the speed of sound of the fuel.

In order to analyze this phenomenon, the temporal evolution of the pressure at the nozzle inlet has been registered and plotted in Figures 13 and 14 for injection pressures of 50 and 150 MPa, respectively, for *ET*=1ms. Considering the small differences existing between the bulk modulus and speed of sound for the two fuels (see Figure 3), it is expected that the pressure waves are considerably similar for both of them. Indeed, this behavior is the one observed for high injection pressures. On the contrary, when injection pressure gets lower there are important deviations between the two waves,

both in terms of amplitude and phase. As it was previously seen, these differences are not justified in terms of fuel properties. Nevertheless, the differences observed can be explained due to the different needle dynamics between the two fuels. As stated before, for low injection pressures the needle velocity is much lower for the biodiesel fuel. This implies that, for the same time, the volume at which the pressure waves are taking place is considerably different, affecting the characteristics of the wave. When injection pressure increases, the injection system shows similar needle velocities for the two fuels tested, and this effect disappears, obtaining the slight variations expected for the effect of fuel properties.

5. PROPOSAL OF A MODIFIED INJECTOR FOR BIODIESEL FUELS

5.1. Simple injection analysis

As it has been seen along this paper, the use of biodiesel fuel has a negative impact on the transient behavior of the injector, especially at low injection pressure. This fact is mainly due to the higher viscosity of the biodiesel fuel with respect to the regular diesel fuel, which implies higher viscous forces on the needle. Nevertheless, it is possible to design a new injector so that its dynamic response when injecting biodiesel is similar to the original one working with regular diesel.

Paying attention to Figure 4, the main difference between the two fuels used consists on the raising slope of the needle lift (and its consequent effect on mass flow rate characteristics). On the contrary, during the closing phase of the injection event both fuels show a similar response once maximum needle lift is obtained (in this case, only for ET=2ms). Thus, it is necessary to propose a modification of the injector that affects only to the opening slope of the injection. From previous experiences [25] [26], it is known that this kind of behavior can be reached by modifying the outlet orifice of the

control volume (orifice OA in Figure 15). If the diameter of this orifice is increased, pressure inside the control volume will fall faster once the solenoid valve is open, leading to a faster needle movement. On the contrary, if the modification was made on the inlet orifice of the control volume (OZ in Figure 15), this would have an impact not only on the opening slope of the needle lift curve, but also on the closing phase of the injection event.

Taking into account this reasoning, 12 simulations have been done using biodiesel as test fluid and varying the diameter of the OA orifice from its original value (0.246 mm) to 0.35 mm, in order to find the configuration that reaches the most similar behavior to the regular diesel fuel. These simulations have been made for the injection pressure of 40 MPa, which has shown to be the most sensitive to fuel properties, and for an energizing time of 1 millisecond. The information obtained from these cases is summarized in Figure 16, where the temporal evolution of the needle lift and the mass flow rate are depicted, together with the deviation of the mass injected between the original configuration of the injector using diesel fuel and the modified one using biodiesel fuel, represented against the OA orifice diameter. Looking at the needle lift plot, it is appreciable that the opening slope and the value of the maximum needle lift increase considerably as OA diameter gets higher. Obviously, this behavior has a significant impact on mass flow rate curve shape, which is more squared when this diameter increases. Additionally, the hydraulic delay is reduced. Comparing these cases to the values obtained for the standard diesel fuel and the original control volume configuration, it is noticeable that the OA diameter which reaches the most similar behavior for needle lift and mass flow rate curves (in comparison to the original configuration) is the one corresponding to the value of D_{OA}=0.27 mm, which implies an increment of 9.75% with respect to the original injection system. Furthermore, if the

deviation between the total mass injected for each of these simulations and the reference case (standard diesel with the original injector configuration) is calculated, the minimum value of this parameter, represented at the bottom and right side of the figure, corresponds also to the 0.27 mm case, as it was expected from the qualitative analysis of the curves.

Figure 17 shows the temporal evolution of pressure inside the control volume for the 12 cases considered in this section. As it was expected, increasing OA diameter implies that the mass flow evacuated by this orifice is higher, leading to a faster and more significant reduction in the control volume pressure. This fact implies that the pressure difference between the top and the bottom of the needle increases, compensating the effect of the viscous forces and leading to a higher needle velocity.

Up to this point, the increment of the OA orifice diameter from the original value of 0.246 mm to 0.27 mm has shown to be useful in order to improve the dynamic response of the injector when using biodiesel fuel at low injection pressure. Nevertheless, it is also important to check that the injection behavior is not significantly modified for high injection pressures, at which both fuels already had similar performances (see Figure 6). For this purpose, one additional case corresponding to a diameter of 0.27 mm and an injection pressure of 180 MPa has been calculated and compared to the original configuration for the two fuels in Figure 18. As it can be observed, the three cases show similar behavior both in terms of needle displacement and instantaneous mass flow rate. Thus, it can be concluded that the proposed modification compensates the strong differences seen at low injection pressure, but not affecting considerably the injector behavior when P_{inj} gets higher.

5.2. Multiple injection analysis

Once the modified configuration for the biodiesel fuel has been obtained and examined for the single injection strategy, it is also interesting to test its behavior for multiple injections. In this sense, an analysis similar to the one developed in the section 3 of the current paper has been done, considering 17 electric dwell times and 4 injection pressure values: 40, 50, 80 and 180 MPa.

Figures 19 and 20 show the comparison of the mass flow rate curves for injection pressures of 40 MPa and 180 MPa, respectively, and 3 different configurations: diesel and biodiesel fuels with the original control volume geometry (i.e., results corresponding to the calculations already analyzed in section 3) and biodiesel fuel with the proposed modification of the injector. For each of these conditions, three mass flow rate curves are depicted, corresponding to the highest and lowest dwell times, as well as the one closest to the critical electric dwell time value (in case that this critical DT exists). As it can be seen, for the case of P_{inj} = 40 MPa the original injector with the biodiesel fuel did not reveal any overlapping phenomenon between the main and the post injection. Furthermore, the masses injected during the pilot injection where extremely low. This behavior is due to the poorer dynamic response of the original injector when using biodiesel. On the contrary, the proposed modification modifies this transient behavior, showing similar mass flow rate curves as seen for the standard diesel fuel. Additionally, for P_{inj} = 180 MPa all the calculations show similar mass flow rate curves, differing only on the stationary values due to the differences in terms of fuel properties.

One important parameter to analyze the behavior of these main plus post injections is the critical dwell time. This information can be seen in Figure 21 for the three configurations tested along the paper. As explained in section 3, at low injection

pressures there is a strong difference in this parameter between the diesel and biodiesel fuel. With the proposed modification, this difference is strongly reduced, leading to slightly higher values of critical DT with respect to the original injector and the diesel fuel. When injection pressure reaches 80 MPa all the configurations achieve similar values.

6. CONCLUSIONS

In this paper a study of the influence of using RME on a standard common-rail injection system has been carried out. This study has been made by means of a one-dimensional model of a solenoid injector, previously developed and validated. The effect of biodiesel properties on the hydraulic behavior of this system has been widely analyzed.

Firstly, a study of the injection system behavior under single shot strategies has been developed. For this purpose, a total of six injection pressure levels and four energizing times have been considered. From these results, several conclusions can be drawn:

- The needle velocity is faster for the standard diesel fuel during the opening phase, especially at low injection pressures. This is a consequence of the higher viscosity of the biodiesel fuel, which increases the friction force, affecting the needle movement.
- Since lower needle lifts are reached with the biodiesel fuel during the transient stages of the injection process, the mass flow rate observed at low energizing times is considerably lower.
- The hydraulic delay is also significantly higher for the biodiesel fuel. The differences are extremely important for the case of injection pressure of 40 MPa. For higher injection pressure values, the differences in terms of hydraulic delay between the fuels have been estimated between 15 and 20 microseconds.

- The mass flow rate measurements at maximum needle lifts obtained for the two fuels are more similar than what would be expected attending to their differences in terms of density. Nevertheless, it is known that the discharge coefficient increases as *Re* gets higher. Due to its higher viscosity, biodiesel shows lower values of Reynolds number for the same pressure conditions, so that the discharge coefficient is significantly lower, especially at low injection pressures. The effect of the discharge coefficient compensates the effect of density, leading to similar stationary mass flow rates.

After this, the development of the injection system under split injection strategies has been characterized for the two fuels. In particular, main plus post injection strategies have been analyzed with injection pulses of 1 and 0.35 ms respectively, leading to the following conclusions:

- For low dwell times it can be seen that main and post injections overlap, so that the mass flow rate curves of the two injection events cannot be distinguished. The characteristic dwell time at which this overlapping stops occurring has been characterized, showing that it is lower for the biodiesel fuel at low injection pressure. This fact is a consequence of the slower needle dynamics for this fuel, which implies that lower needle lifts are reached for this fuel, so that the injector closes at lower times.
- The main injection has shown to have an effect on the amount of fuel injected during the post injection event. Furthermore, it has been observed that the post injections are considerably higher in terms of mass for the diesel fuel. Nevertheless, this difference decreases as injection pressure gets higher.
- The oscillatory characteristics of the pressure at the nozzle inlet are similar for the two fuels due to the low differences observed between them in terms of bulk

modulus and speed of sound. Nevertheless, for low injection pressures (up to 50 MPa) the significant influence of fuel properties on needle dynamics produces an impact in the amplitude and the phase of the pressure wave.

Finally, a modification of the injector geometry has been proposed for the biodiesel fuel in order to have a behavior similar to the one obtained for the original injector for the standard diesel. In order to improve the dynamic response of the injector, especially at low injection pressure, the diameter of the outlet orifice of the control volume has been increased. As a consequence, pressure at the control volume during the opening phase of the injection event is considerably reduced, leading to faster needle movement. From the different values tested, it has been obtained that the optimal diameter is around 0.27 mm, which implies an increment of 9.75% with respect to its original value. Additionally, this proposed configuration has been tested for a high injection pressure case, leading to similar performances as found for the original configuration. Finally, main plus post injection strategies have been tested for this modified injector, showing results that are very similar to the ones obtained for the original injector with the standard diesel fuel, both in terms of mass flow rate evolution and critical dwell time.

ACKNOWLEDGEMENTS

This work was sponsored by “Vicerrectorado de Investigación, Desarrollo e Innovación” of the “Universidad Politécnica de Valencia” in the frame of the project “Estudio numérico de la cavitación en toberas de inyección Diesel mediante Grid Computing (Cavigrid) ”, Reference Nº 2597 and by “Ministerio de Ciencia e Innovación” in the frame of the Project “Estudio teórico experimental sobre la influencia del tipo de combustible en los procesos de atomización y evaporación del

chorro Diesel (PROFUEL)", reference TRA2011-26293. This support is gratefully acknowledged by the authors.

REFERENCES

[1] M. Zheng, R. Kumar, Implementation of multiple-pulse injection strategies to enhance the homogeneity for simultaneous low-NOx and -soot diesel combustion, Int. J. Therm. Sci. 48 (2009) 1829-1841.

[2] M. Yao, H. Wang, Z. Zheng, Y. Yue, Experimental study of n-butanol additive and multi-injection on HD diesel engine performance and emissions, Fuel 89 (2010) 2191-2201.

[3] H.K. Suh, S.H. Yoon, C.S. Lee, Effect of Multiple Injection Strategies on the Spray Atomization and Reduction of Exhaust Emissions in a Compression Ignition Engine Fueled with Dimethyl Ether (DME), Energ. Fuel 24 (2010) 1323-1332.

[4] R. Altin, S. Cetinkaya, H.S. Yucescu, The potential of using vegetable oil fuels as fuel for diesel engines, Energ. Convers. Manage. 42(5) (2001) 529-538.

[5] C.D. Rakopoulos, K.A. Antonopoulos, D.C. Rakopoulos, D.T. Hountales, E.G. Giakoninis, Comparative performance and emissions study of a direct injection Diesel engine using blends of Diesel fuel with vegetable oils or bio-diesels of various origins, Energ. Convers. Manage. 47 (18-19) (2006) 3272-3287.

[6] A. K. Agarwal, Biofuels (alcohols and biodiesel) applications as fuels for internal combustion engines, Prog. Energ. Combust. 33 (3) (2007) 233-271.

[7] D.H. Qi, H. Chen, L.M. Geng, Experimental studies on the combustion characteristics and performance of a direct injection engine fueled with biodiesel/diesel blends, Energ. Convers. Manage. 51(12) (2010) 2985-2992.

[8] Ozsecen, A.N. and Canakci, M., Determination of performance and combustion characteristics of a diesel engine fueled with canola and waste palm oil methyl esters, Energ. Convers. Manage 52 (1) (2011) 108-116.

[9] S.A. Basha, K.R. Gopal, S. Jebaraj, A review on biodiesel production, combustion, emissions and performance, Renew. Sust. Energ. Rev. 13 (6-7) (2009) 1628-1634.

[10] M. Lapuerta, O. Armas, J. Rodríguez-Fernández, Effect of biodiesel fuels on diesel engine emissions, Prog. Energ. Combust. 34(2) (2008): 198-223.

[11] F. Boudy, P. Seers, Impact of physical properties of biodiesel on the injection process in a common-rail direct injection system, Energ. Convers. Manage. 50 (12) (2009) 2905-2912.

[12] N.H. Chung, B.H. Oh, M.H. Sunwoo, Modelling and injection rate estimation of common-rail injectors for direct-injection diesel engines, P. I. Mech. Eng. D-J. Aut. 222 (2008) 1089-1101.

[13] R. Payri, H. Climent, F.J. Salvador, A.G. Favennec, Diesel injection system modelling. Methodology and application for a first-generation common rail system, P. I. Mech. Eng. D-J. Aut.218 (2004) 81-91.

[14] F. Payri, V. Bermúdez, R. Payri, F.J. Salvador, The influence of cavitation on the internal flow and the spray characteristics in diesel injection nozzles, Fuel83 (2004) 419-431.

[15] K. Jung, T. Khil, Y. Yoon, Effects of orifice internal flow on breakup characteristics of like-doublet injectors, J. Propul. Power 22(3) (2006) 1329-1339.

[16] S. H. Park, H.K. Suh, C.S. Lee, Effect of cavitating flow on the flow and fuel atomization characteristics of biodiesel and diesel fuels, Energ. Fuels 22 (2008) 605-613.

[17] A. Sou, S. Hosokawa, A. Tomiyama, Effects of cavitation in a nozzle on liquid jet atomization. Int. J. Heat Mass Tran. 50 (2007) 3575-3582.

[18] L.C. Ganipa, S. Andersson, J. Chomiak, Combustion characteristics of Diesel sprays from equivalent nozzles with sharp and rounded inlet geometries, Combust. Sci. Tech. 175 (2003) 1015-1032.

[19] M. Costa, B.M. Vaglieco, F.E. Corcione, Radical species in the cool-flame regime of diesel combustion: a comparative numerical and experimental study. Exp. Fluids 39 (2005) 512–524.

[20] R. Payri, F.J. Salvador, J. Gimeno, J. De la Morena, Effects of nozzle geometry on direct injection diesel engine combustion process, Applied Thermal Engineering 29 (2009) 2051–2060.

[21] R. Payri, F.J. Salvador, P. Martí-Aldaraví, J. Martínez-López, Using one-dimensional modelling to analyse the influence of the use of biodiesels on the dynamic behavior of solenoid- operated injectors in common rail systems: detailed injection system model, Energ. Convers. Manage. (2011).

[22] V. Macián, V. Bermúdez, R. Payri, J. Gimeno, New technique for determination of internal geometry of a Diesel nozzles with the use of silicone methodology, Exp. Techniques 27(2003) 39-43.

[23] R. Payri, F.J. Salvador, J. Gimeno, J. De la Morena, Study of cavitation phenomena based on a technique for visualizing bubbles in a liquid pressurized chamber. Int. J. Heat Fluid Fl. 3 (2009) 768-777.

[24] V. Macián, R. Payri, X. Margot, F.J. Salvador, A CFD analysis of the influence of diesel nozzle geometry on the inception of cavitation. Atom Spray 13 (5-6) (2003) 579-604.

[25] J.M. Desantes, J. Arrègle, P.J. Rodríguez. Computational model for simulation of Diesel injection systems. SAE 1999-01-0915, 1999.

[26] R. Payri, Tormos, B., F.J. Salvador, A.H. Plazas.Using one-dimensional modelling codes to analyse the influence of diesel nozzle geometry on injection rate characteristics. International Journal of vehicle design 38 (2005) 58-78.

TABLES

Table 1: diesel fuel and RME properties considered for the model

Fuel	**Density (at 30°C) [kg/m^3]** *(EN ISO 12185/96)*	**Viscosity (at 30 °C) [kg/m·s]** *(EN ISO 3104/99)*
Diesel	825.3	$2.8031 \cdot 10^{-3}$
RME	865	$4.9 \cdot 10^{-3}$

FIGURE CAPTIONS

Figure 1: scheme of the injector model

Figure 2: validation of the injector model with experimental mass flow rate curves

Figure 3: Bulk modulus and speed of sound for the diesel and biodiesel fuel in terms of injection pressure.

Figure 4: Needle lift and injection rate for diesel and biodiesel fuel. P_{inj} = 40 MPa.

Figure 5: Needle lift and injection rate for diesel and biodiesel fuel. P_{inj} = 80 MPa.

Figure 6: Needle lift and injection rate for diesel and biodiesel fuel. P_{inj} = 180 MPa.

Figure 7: Difference of hydraulic delay between RME and regular diesel fuel in terms of injection pressure.

Figure 8: Evolution of the discharge coefficient with respect to Reynolds number.

Figure 9: Injection rate for the main plus post strategy. P_{inj} = 50 MPa.

Figure 10: Injection rate for the main plus post strategy. P_{inj} = 120 MPa.

Figure 11: Evolution of the critical electric dwell time in terms of injection pressure.

Figure 12: Mass injected during the post injection for the two fuels and three different injection pressures: 50, 80 and 180 MPa.

Figure 13: Pressure at the nozzle inlet for the two fuels. P_{inj} = 50 MPa.

Figure 14: Pressure at the nozzle inlet for the two fuels. P_{inj} = 150 MPa.

Figure 15: Geometry of the control volume of the injector.

Figure 16: Results of the simulations corresponding to the variation of OA orifice diameter. P_{inj} = 40 MPa.

Figure 17: Temporal evolution of pressure at the control volume for the simulations corresponding to the variation of OA orifice diameter. P_{inj} = 40 MPa.

Figure 18: Results of the simulations corresponding to the variation of OA orifice diameter. P_{inj} = 180 MPa.

Figure 19: Mass flow rate curves using main plus post injection strategy for diesel and biodiesel fuels at the original injector and for the biodiesel fuel at the modified injector. P_{inj} = 40 MPa.

Figure 20: Mass flow rate curves using main plus post injection strategy for diesel and biodiesel fuels at the original injector and for the biodiesel fuel at the modified injector. P_{inj} = 160 MPa.

Figure 21: Evolution of the critical dwell time in terms of injection pressure including the modified injector configuration.

FIGURES

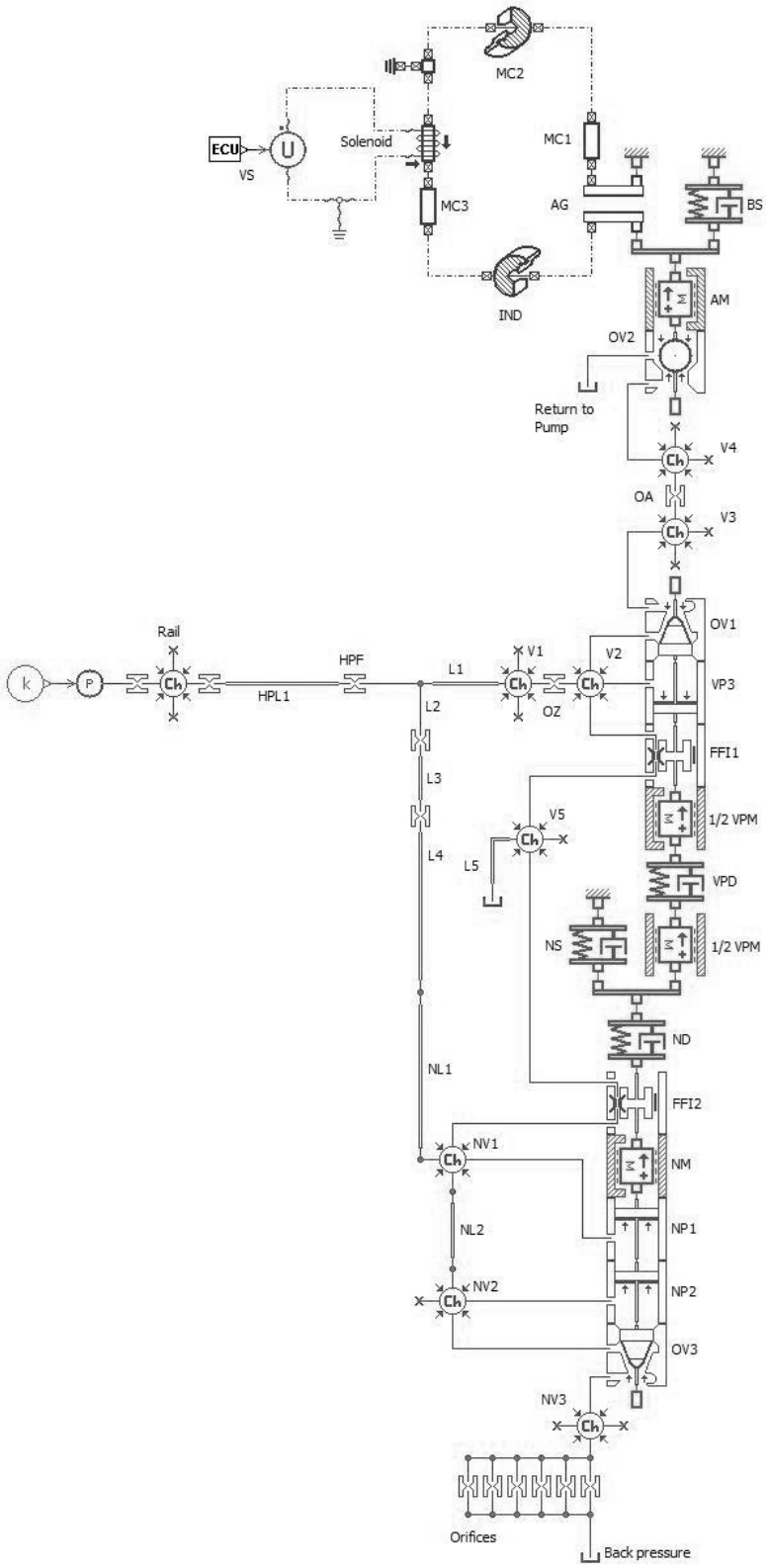

Figure 1: scheme of the injector model

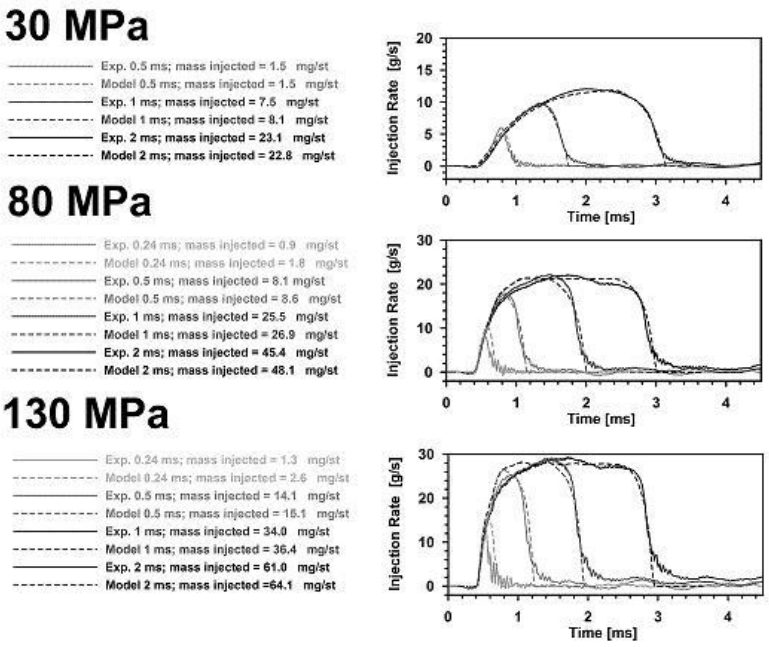

Figure 2: validation of the injector model with experimental mass flow rate curves

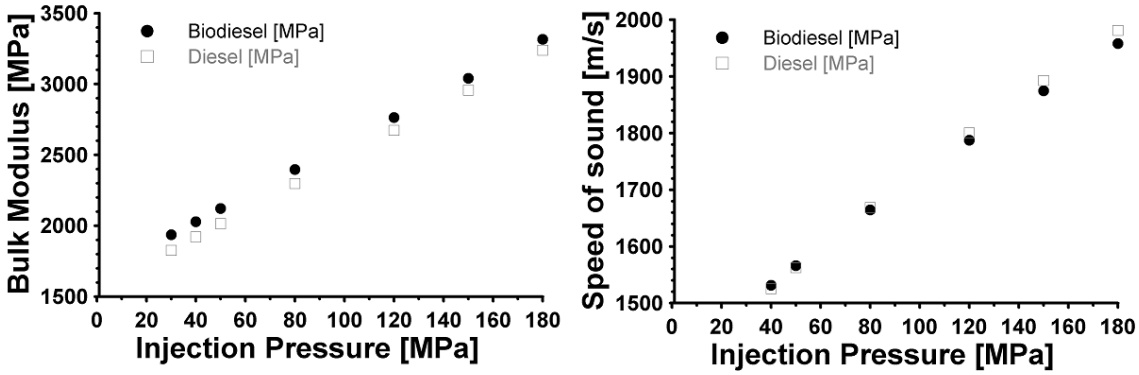

Figure 3: Bulk modulus and speed of sound for the diesel and biodiesel fuel in terms of injection pressure.

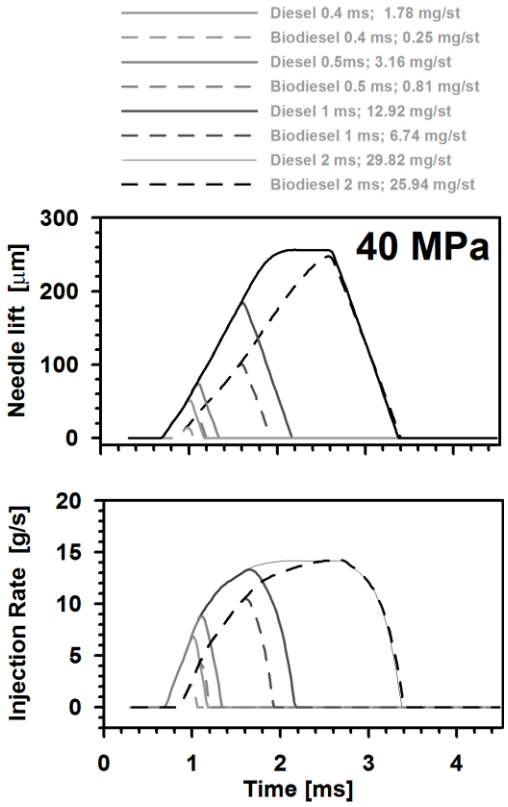

Figure 4: Needle lift and injection rate for diesel and biodiesel fuel. P_{inj} = 40 MPa.

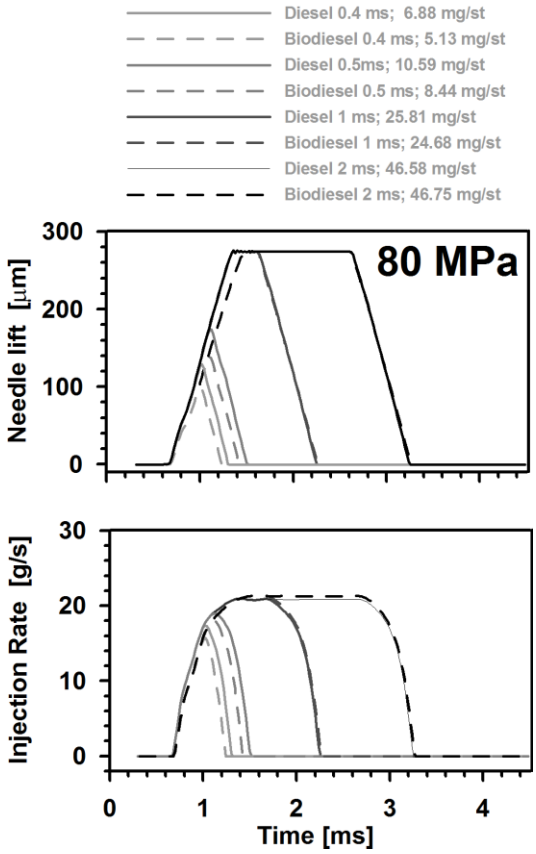

Figure 5: Needle lift and injection rate for diesel and biodiesel fuel. P_{inj} = 80 MPa.

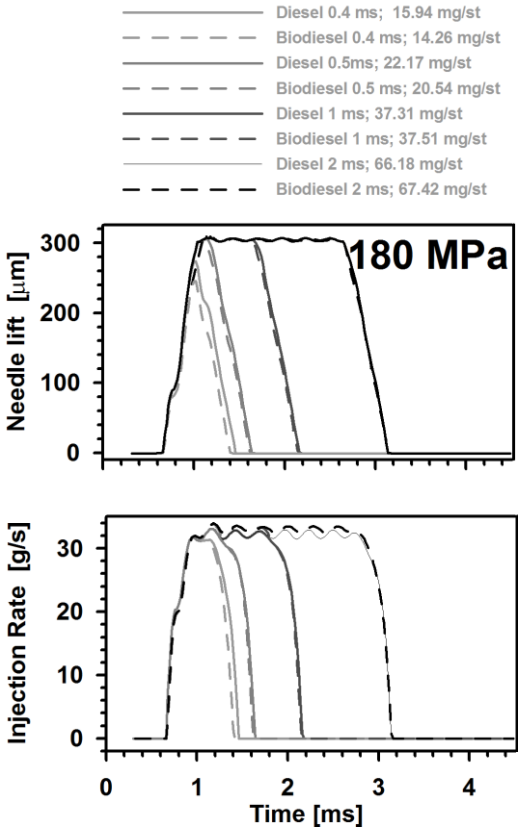

Figure 6: Needle lift and injection rate for diesel and biodiesel fuel. P_{inj} = 180 MPa.

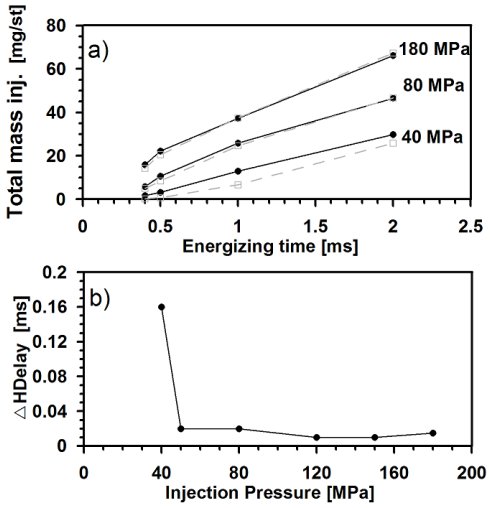

Figure 7: a) total injected mass against energizing time for diesel and biodiesel fuel b) difference of hydraulic delay between RME and regular diesel fuel in terms of injection pressure.

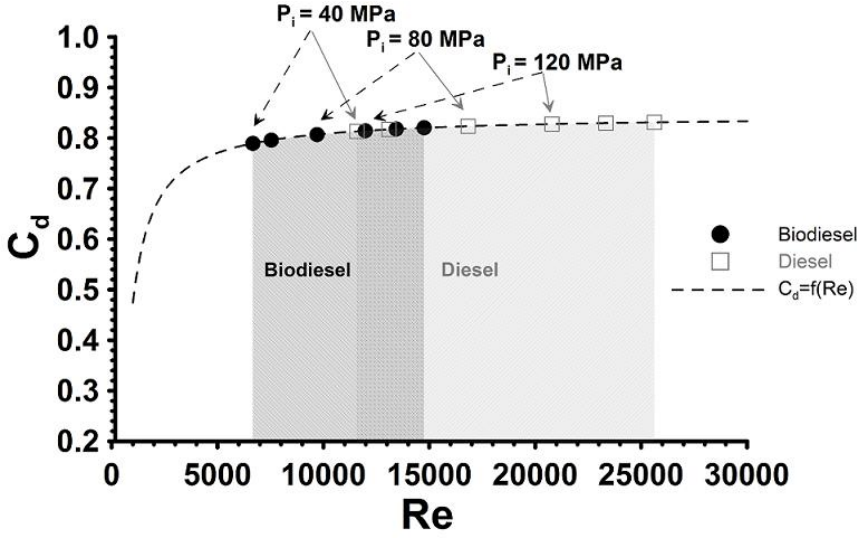

Figure 8: Evolution of the discharge coefficient with respect to Reynolds number

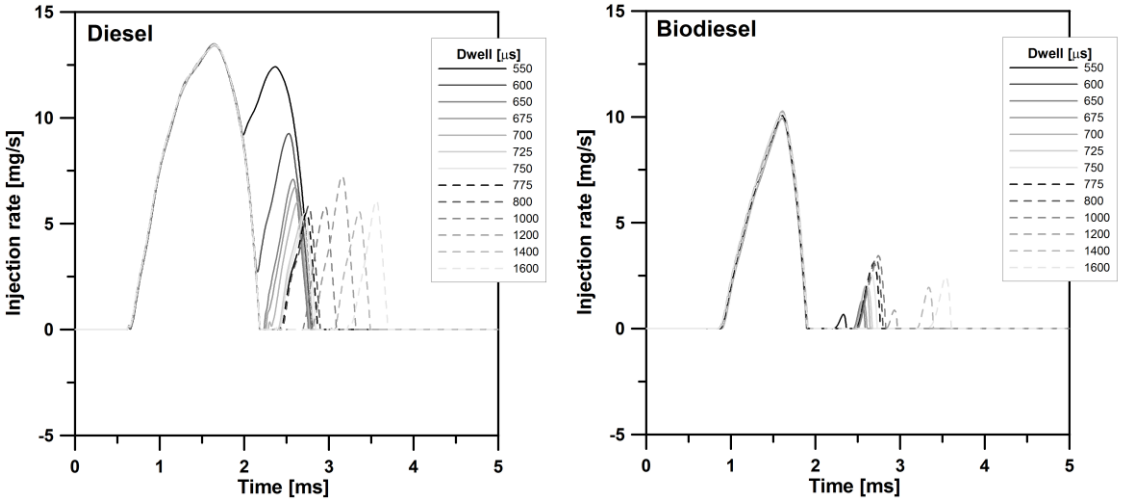

Figure 9: injection rate for the main plus post strategy. P_{inj} = 40 MPa.

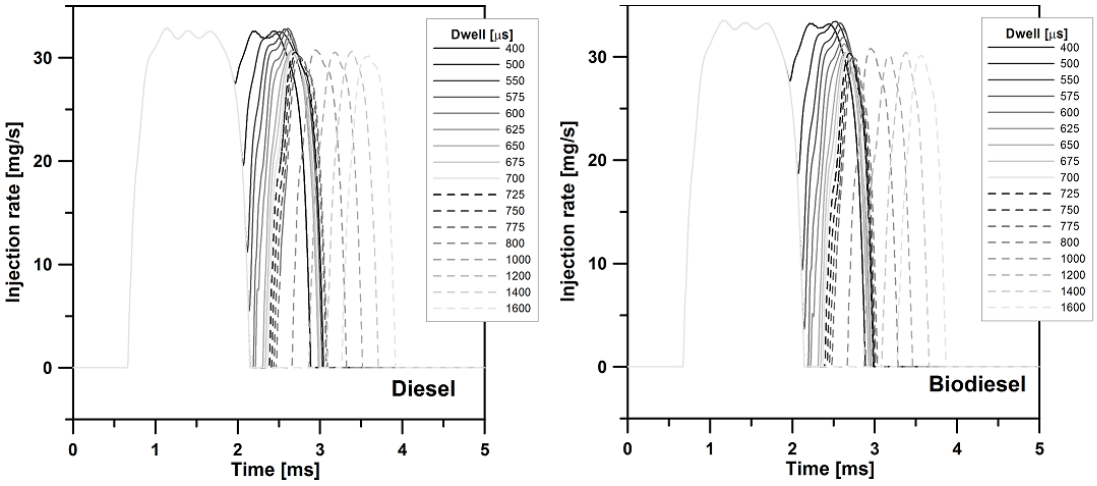

Figure 10: injection rate for the main plus post strategy. P_{inj} = 180 MPa.

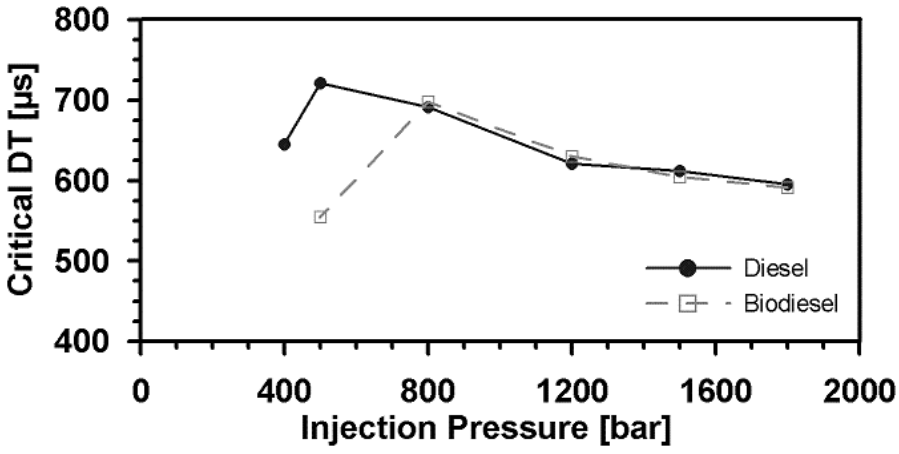

Figure 11: evolution of the critical dwell time in terms of injection pressure.

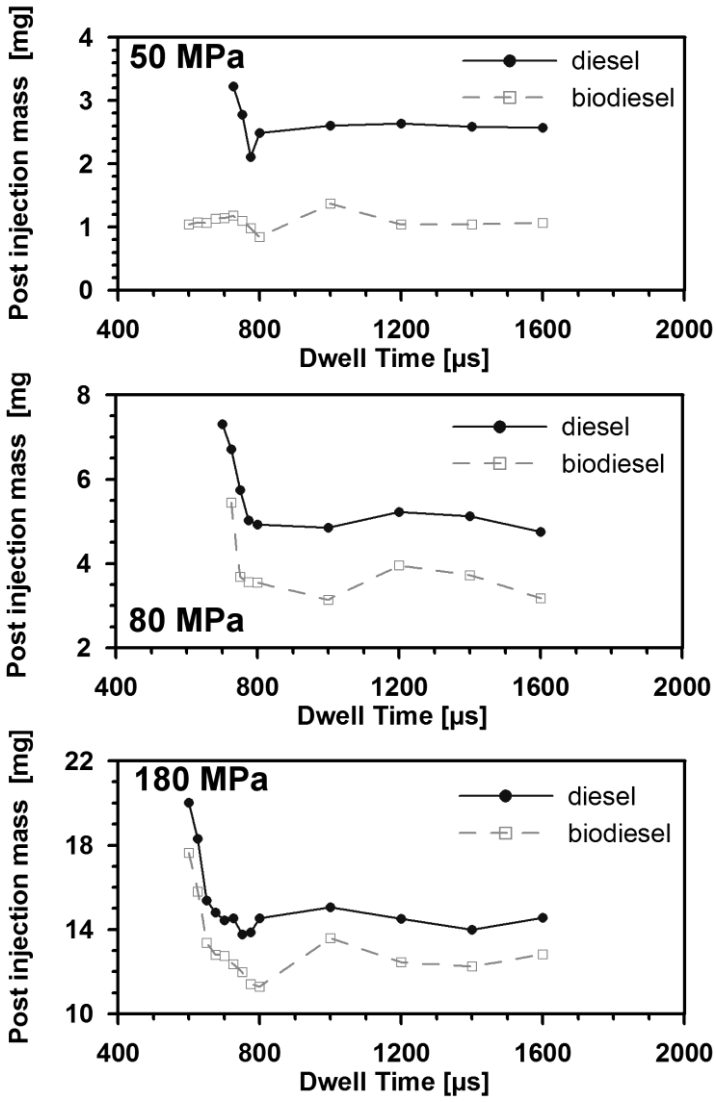

Figure 12: mass injected during the post injection for the two fuels and three different injection pressures: 50, 80 and 180 MPa.

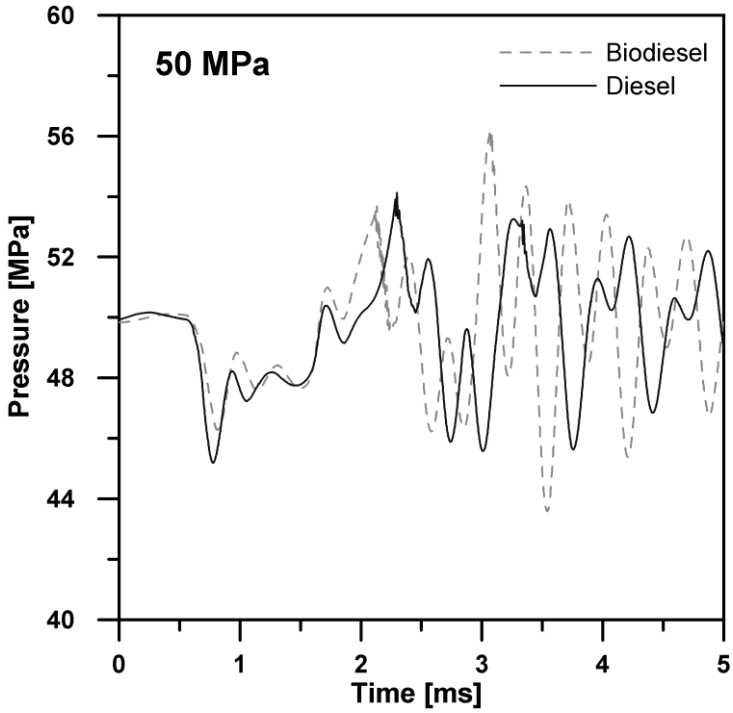

Figure 13: pressure at the nozzle inlet for the two fuels. P_{inj} = 50 MPa.

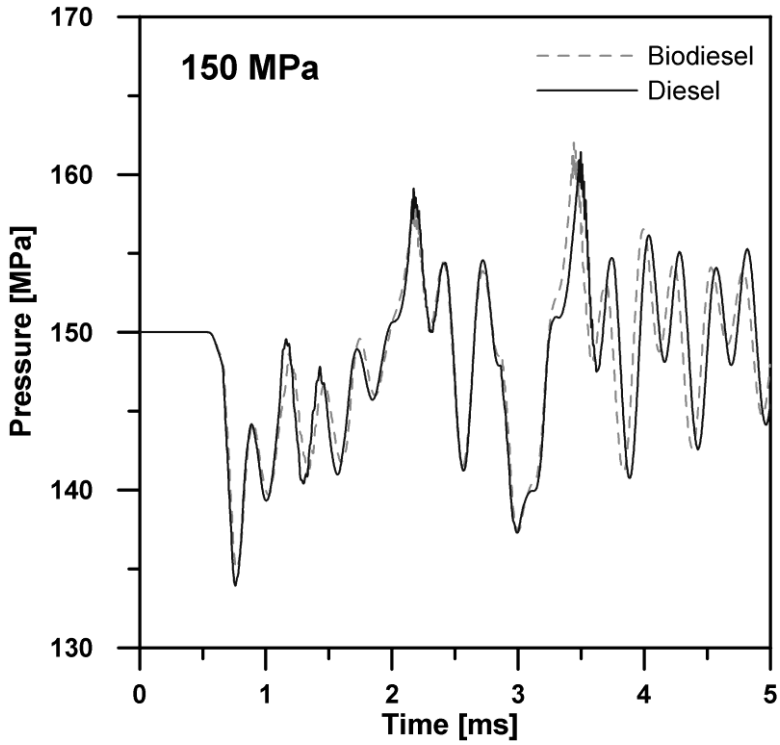

Figure 14: pressure at the nozzle inlet for the two fuels. P_{inj} = 150 MPa.

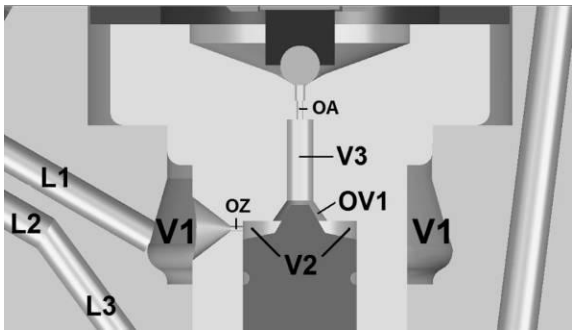

Figure 15: geometry of the control volume of the injector.

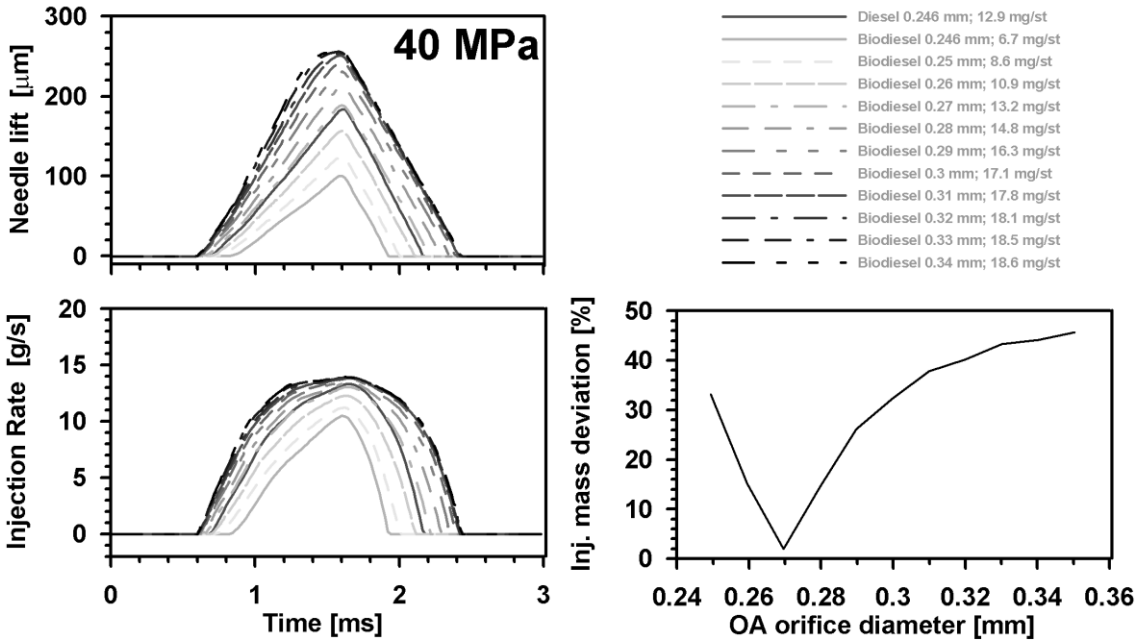

Figure 16: Results of the simulations corresponding to the variation of OA orifice diameter. P_{inj} = 40 MPa

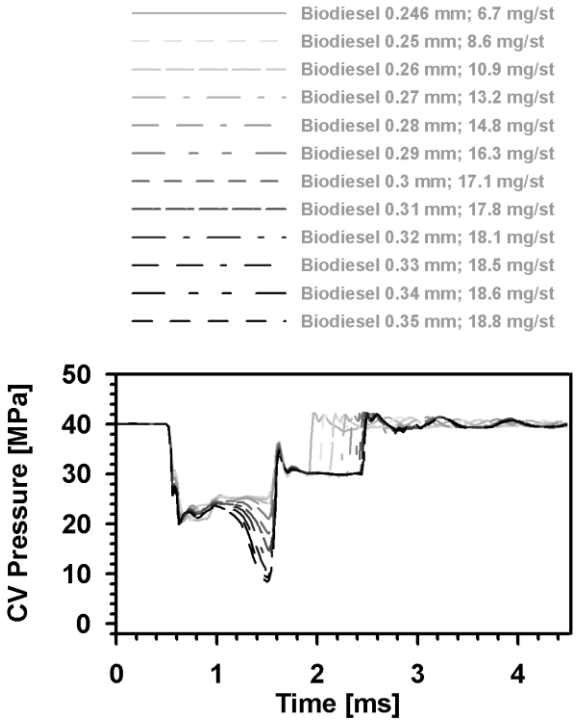

Figure 17: temporal evolution of pressure at the control volume for the simulations corresponding to the variation of OA orifice diameter. P_{inj} = 40 MPa

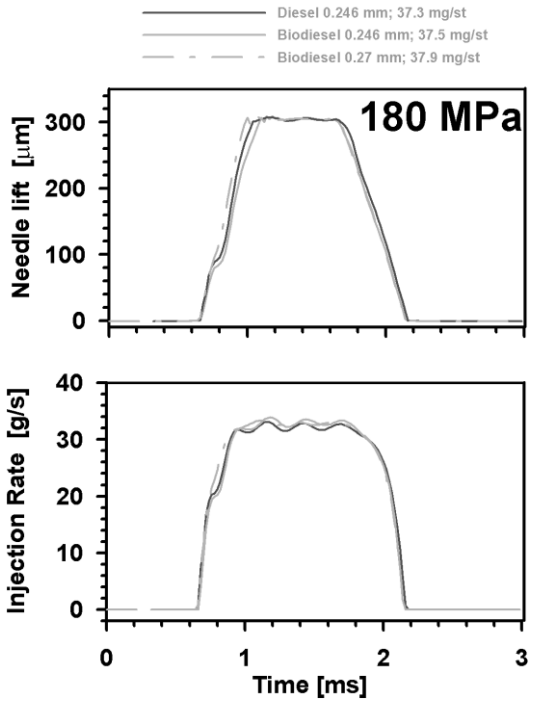

Figure 18: Results of the simulations corresponding to the variation of OA orifice diameter. P_{inj} = 180 MPa

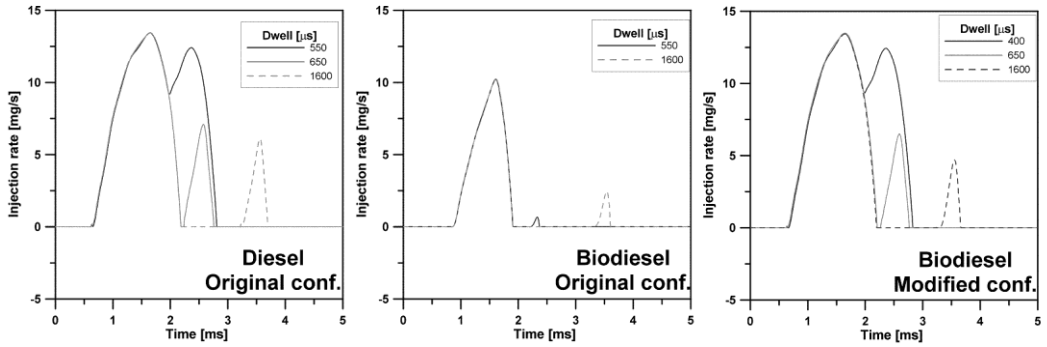

Figure 19: Mass flow rate curves using man plus post injection strategy for diesel and biodiesel fuels at the original injector and for the biodiesel fuel at the modified injector. P_{inj} = 40 MPa.

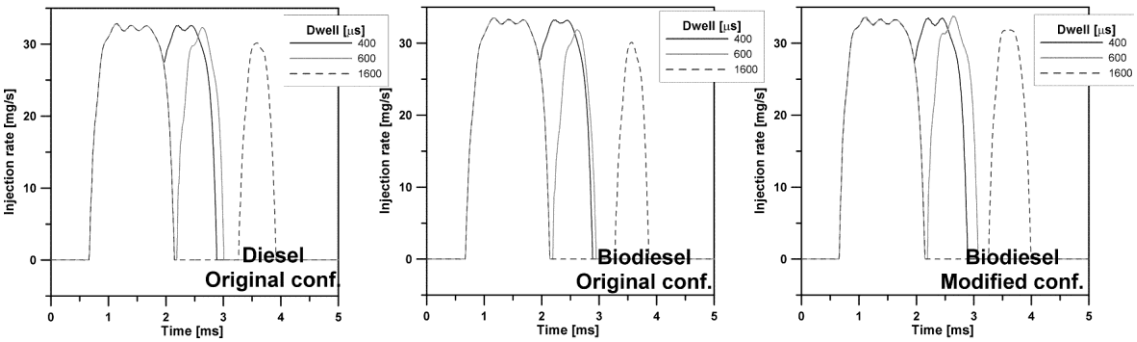

Figure 20: Mass flow rate curves using man plus post injection strategy for diesel and biodiesel fuels at the original injector and for the biodiesel fuel at the modified injector. P_{inj} = 180 MPa.

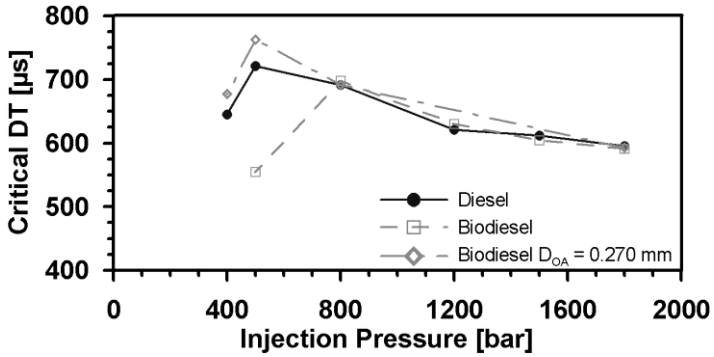

Figure 21: evolution of the critical dwell time in terms of injection pressure including the modified injector configuration.